Sensors & Transducers Journal, Vol. 12, Special Issue, October 2011, pp. 71-79

www.sensorsportal.com

Sensors & Transducers

ISSN 1726-5479

http://www.sensorsportal.com

Dynamic- and Thermo-mechanical Analysis of Inorganic Nanotubes/elastomer Composites

[1] Armin FUITH, [1] Marius REINECKER, [2] Antoni SÁNCHEZ-FERRER, [2] Raffaele MEZZENGA, [3] Aleš MRZEL, [4] Maris KNITE, [5] Ilze AULIKA, [6] Marija DUNCE and [1] Wilfried SCHRANZ

[1] University of Vienna, Functional Materials, Boltzmanngasse 5, A-1090 Vienna, Austria
[2] ETH Zurich, Institute of Food, Nutrition & Health, Food & Soft Materials Science Group, Schmelzbergstrasse 9, LFO, E23-E29, CH-8092 Zurich, Switzerland
[3] J. Stefan Institute, Jamova 39, SI 1000 Ljubljana, Slovenia
[4] Institute of Technical Physics, Riga Technical University, Azenes Str. 14/24, LV-1048, Riga, Latvia
[5] Center for Space Human Robotics – IIT@Polito, Corso Trento 21, 10129, Turin, Italy
[6] Institute of Solid State Physics, University of Latvia, Kengaranga Str. 8, LV-1063, Riga, Latvia
E-mail: armin.fuith@univie.ac.at, marius.reinecker@univie.ac.at, wilfried.schranz@univie.ac.at, antoni.sanchez@agrl.ethz.ch, raffaele.mezzenga@agrl.ethz.ch, ales.mrzel@ijs.si, knite@latnet.lv, ilze.aulika@iit.it, mdunce@gmail.com

Received: 15 June 2011 /Accepted: 18 July 2011 /Published: 31 October 2011

Abstract: We present dynamic mechanical analysis (DMA) and thermomechanical analysis (TMA) measurements of a new type of polyurea elastomer nanocomposites based on inorganic MoS_2 nanotubes and $Mo_6S_2I_8$ nanowires. The addition of a small amount of nanoparticles (<1 wt-%) leads to an increase of the glass transition temperature T_g as compared to the pure elastomeric matrix. A second peak observed in tanδ in the pure and mixed elastomer is attributed to a second glass transition occurring in regions near the hard nanodomains of the microphase separated polyurea system. It is also found that the small amount of nanoparticles leads to an increase in the Young´s modulus of up to 15 % in the whole measured temperature range (from -130 °C to 20 °C). The thermal expansion of doped samples is considerably larger above T_g. Below T_g, this difference vanishes completely. A very similar behaviour was also found in measurements of polyisoprene/multiwall carbon nanotube (MWCNT) composites. *Copyright © 2011 IFSA.*

Keywords: Inorganic nanotubes, Polymer nanocomposites, Dynamic mechanical analysis, Thermomechanical analysis, Glass transition, Elastomer, Polyurea.

1. Introduction

Polymer nanostructured composites have gained much interest due to their potential use as flexible large size sensors with superior mechanical and/or electrical properties [1]. TMA (thermomechanical analysis) and DMA (dynamic mechanical analysis) were performed to study thermal expansion, as well as temperature and frequency dependence on the nanostructured composite materials. In this work we present recent results based on TMA and DMA measurements on the nanotubes/elastomer (MoS_2) and nanowires/elastomer ($Mo_6S_2I_8$) nanocomposites. The polyurea matrix was chosen as the reference elastomeric system in order to compare the effect due to the presence of nanoparticles in the matrix. Polyurea synthesis is similar to the one used for polyurethane, which was introduced in 1937 by Otto Bayer for replacement of natural rubber. Polyurea is an attractive material with many applications such as coatings, implants or medical devices. It forms by the rapid reaction of isocyanates (rigid molecules) with polyetheramines (flexible chains). Polyurea exhibits a phase separated structure with rigid urea domains (hard domains) embedded in a matrix of flexible polymer chains (soft domains) [2-4]. The mechanical properties of polyurea can be tuned over a broad range by varying the molecular weight of the components, the relative amount of hard and soft domains, and the loading of nanoparticles [3, 4]. In the present work, we study the influence of inorganic nanotubes (MoS_2) [5] and nanowires ($Mo_6S_2I_8$) [6] to the mechanical properties and to the glass transition temperature in the polyurea matrix. The results are compared to recent measurements on polyisoprene/multiwall carbon nanotube (MWCNT) composites [7].

2. Experimental Part

2.1. Samples Preparation

Three elastomers were synthesized: a reference elastomer (PU) without any nanoparticle, and two elastomer nanocomposites containing nanotubes (PU-MoS_2) and nanowires (PU-$Mo_6S_2I_8$). For the synthesis of the three elastomers, two solutions in acetone were prepared as described in literature [2-4]: one containing the diamino-terminated polymer, and the other the trifunctionalized crosslinker with or without nanoparticles. In order to obtain a final solid content of 15% w/v, 3.85 g of Jeffamine D-2000 (Hunstman) was dissolved in 11.1 mL of acetone, and 0.65 g of Basonat HI-100 (BASF) was dissolved in 14.5 mL of acetone. In the case of elastomers containing nanoparticles, the Basonat HI-100 was dissolved in an ultrasonicated acetone dispersion of the corresponding nanoparticles to be incorporated. The two solutions were mixed and gently stirred for 5 min, and the final solution was cast onto the glass surface of a Petri dish. One day after the samples were cast, the obtained film was allowed to dry in the atmosphere and peeled from the surface. Samples were cut from their corresponding free-standing films ($14.6 \times 5.0 \times 0.75$ mm^3). The final concentration of nanoparticles was less than 1 wt-%.

2.2. Experimental Methods

Dynamic mechanical analysis (DMA) is one of the most commonly applied methods for the determination of the mechanical properties of materials, together with thermomechanical analysis (TMA) for the determination of the thermal expansion. Materials such as polymers and polymer networks can be characterized as a function of temperature and frequency. The complex elastic compliance can be measured in a frequency range from 0.01 Hz to 100 Hz, and for temperatures between 80 K and 850 K.

The principle of the DMA technique is based on the sinusoidally modulated dynamic force $F_{dyn}e^{i\omega t}$ at a chosen amplitude and frequency when applying a static force F_{stat}. The resulting amplitude u and phase shift δ of the resulting elastic response of the sample are registered via inductive coupling with a resolution of $\Delta u \approx 10$ nm and $\Delta\delta \approx 0.1°$. The knowledge of u and δ allows determining the real and imaginary parts of a certain component of the complex elastic compliance tensor S_{ii}

$$S_{ii}' = S_{ii}\cos\delta \text{ and } S_{ii}'' = S_{ii}\sin\delta \quad (1)$$

The inverse compliances are the so-called storage ($E'=1/S_{ii}'$) and loss ($E''=1/S_{ii}''$) modulus. We employ two different kinds of DMA instruments: the Perkin Elmer DMA 7 and the Perkin Elmer Diamond DMA. Table 1 compares the specifications of both instruments as commercially available.

Table 1. Specifications of the Perkin Elmer DMA 7 and the Perkin Elmer Diamond DMA.

	DMA 7	**Diamond DMA**
F_{stat} (maximal force)	2.5 N	10 N
ΔF (resolution)	10^{-5} N	10^{-5} N
ω (frequency range)	0.01 Hz – 50 Hz	0.01 Hz – 100 Hz
T (temperature range)	90 K – 850 K	120 K – 850 K

The minimal force that can be applied in both instruments is 10^{-3} N. The force is transmitted by a rod, which is also the probe for the position of the upper end of the sample. The Perkin Elmer DMA-7 can work with quartz or steel rods and sample holders, whereas the Perkin Elmer Diamond DMA works only with steel holders, which has restricted low temperature performance. The presently used geometries are the parallel plate stress (PPS) and the tensile stress (TS) arrangements as shown in Fig. 1.

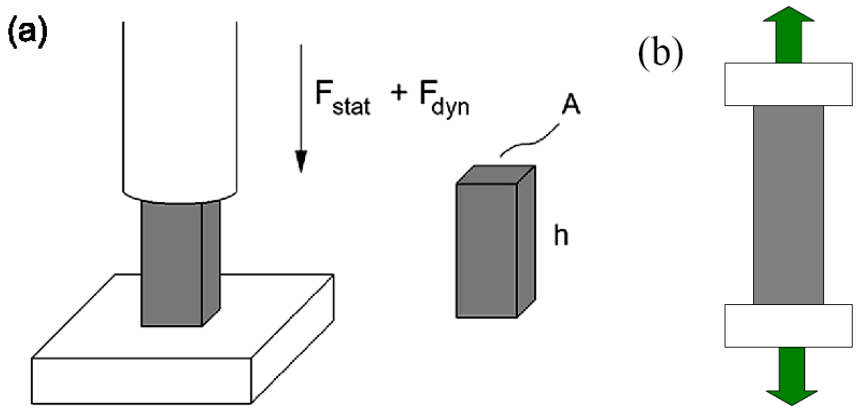

Fig. 1. Typical sample geometries for the PPS (a), and the TS (b) methods.

In PPS geometry, a force F_3 is applied in the z-direction, and the corresponding change in length Δh in the same direction is measured. This yields the Young's or elastic modulus of the sample in the elastic regime $E \equiv 1/S_{33}$. The strain ε_3 is defined as the ration between the change in length with respect to the initial length of the sample $\varepsilon_3 = \Delta h/h$, and the measured stress σ_3 as the applied force divided by the cross section of the element $\sigma_3 = F_3/A$. In the elastic region (for small deformations), both magnitudes are connected by the Young's modulus:

$$\sigma_3 = E\ \varepsilon_3 = 1/S_{33}\ \varepsilon_3 \tag{2}$$

In this way, the effective spring constant of a material $k = F_3/\Delta h = 1/S_{33}\ A/h$ is measured [8, 9].

The Perkin Elmer TMA uses a similar measuring principle as the Perkin Elmer DMA, i.e. the sample position is measured via inductive coupling at nominally zero applied force. The sample geometry is usually the same as for the PPS method (Fig. 1a). A small static force of 10^{-3} N was applied to keep good mechanical contact between the quartz or steel rod and the sample for all our TMA measurements.

3. Results

3.1. TMA Experiments

TMA experiments were carried out in order to analyze the differences in the thermal expansion of both nanocomposites with respect to the pure elastomer matrix. Fig. 2 shows the temperature dependence of the thermal expansion of the pure polyurea system (PU) and the two polyurea nanocomposites PU-MoS_2 and PU-$Mo_6S_2I_8$.

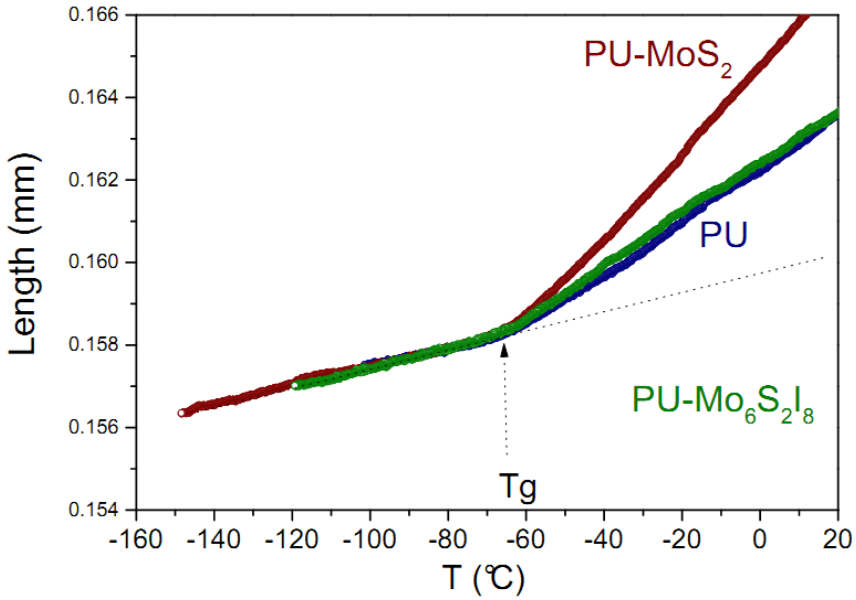

Fig. 2. Thermal expansion as function of temperature for the pure polyurea elastomer (PU), and the polyurea nanocomposites (PU-MoS_2 and PU-$Mo_6S_2I_8$). The curves are normalized to the length of the PU at -120 °C.

Above T_g, the thermal expansion of the nanocomposite PU–MoS_2 is considerably increased, whereas the thermal expansion below T_g is not affected by the presence of the nanotubes (Table 2). This behaviour is very similar to the one found in polyisoprene/multiwall carbon nanotube (MWCNT) and polyisoprene/carbon black (CB) composites as shown in Fig. 3. The nanowires containing nanocomposite (PU-$Mo_6S_2I_8$) has a similar behaviour than the pure polyurea matrix. It seems that nanowires do not affect that much the thermal properties of the polymer matrix.

Table 2. Linear thermal expansion coefficients $\alpha_L = (1/L_0)(\Delta L/\Delta T)$ of PU, PU-MoS_2 and PU-$Mo_6S_2I_8$ calculated from Fig. 2 with $L_0 = L(T = -120\ °C)$. The volume thermal expansion coefficient is $\alpha = 3\alpha_L$.

	$\alpha_L(T < T_g)$	$\alpha_L\ (T > T_g)$
PU, PU $Mo_6S_2I_8$	1.3 10^{-4} K^{-1}	3.9 10^{-4} K^{-1}
PU-MoS_2	1.3 10^{-4} K^{-1}	6.5 10^{-4} K^{-1}

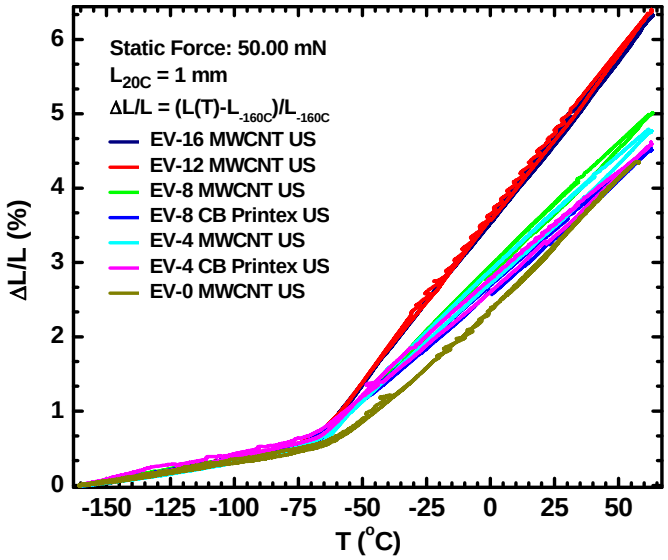

Fig. 3. Relative length $\Delta L/L$ ($\Delta L/L = L(T) - L(T = -160\ °C)/L(T = -160\ °C)$) as function of temperature for the polyisoprene/multiwall carbon nanotube (MWCNT) and polyisoprene/carbon black (CB) nanocomposites.

The thermal expansion coefficient α of polymer nanocomposites depends on many factors: the type of interaction between the nanoparticles and the polymer backbones, the shape of the nanoparticles, the volume fraction of the nanoparticles, and the thermal expansion coefficient of the nanoparticles [19]. Since some of these ingredients like the thermal expansion coefficient of MoS_2 and $Mo_6S_2I_8$ are not yet known, a quantitative analysis of the present thermal expansion data has to wait for a future work.

3.2. DMA Experiments

DMA experiments were performed for the determination of the Young's modulus and tanδ as function of temperature, as well as the glass transition temperatures upon heating the sample. Fig. 4 shows the temperature dependences of the real (E') and the imaginary (E") part of the complex Young's modulus of pure polyurea (PU) and the two polyurea nanocomposites (PU-MoS_2 and PU-$Mo_6S_2I_8$). The measurements were performed in TS mode at 1 Hz frequency, with a strain rate of $d\varepsilon/dt = 0.1\ s^{-1}$. Recently performed DMA measurements on polyurea/polyurethane systems at 1 Hz [10] show a very similar behaviour, where in addition to the $T_{g\alpha}$ around –47 °C some elastic anomalies at $T_{g\beta} = -80$ °C and $T_{g\gamma} = -141$°C were found, whose origins are not yet clear.

With the addition of nanotubes (MoS_2) and nanowires ($Mo_6S_2I_8$), a clear upwards shift in the glass transition temperature can be observed from the decays in the storage modulus (E') and the maxima in the loss modulus (E") of both nanocomposite samples. The same tendency has been also obtained by analyzing the thermal expansion data in Fig. 2. The results are summarized in Table 3. A possible origin for this increase of T_g with filler content will be discussed below.

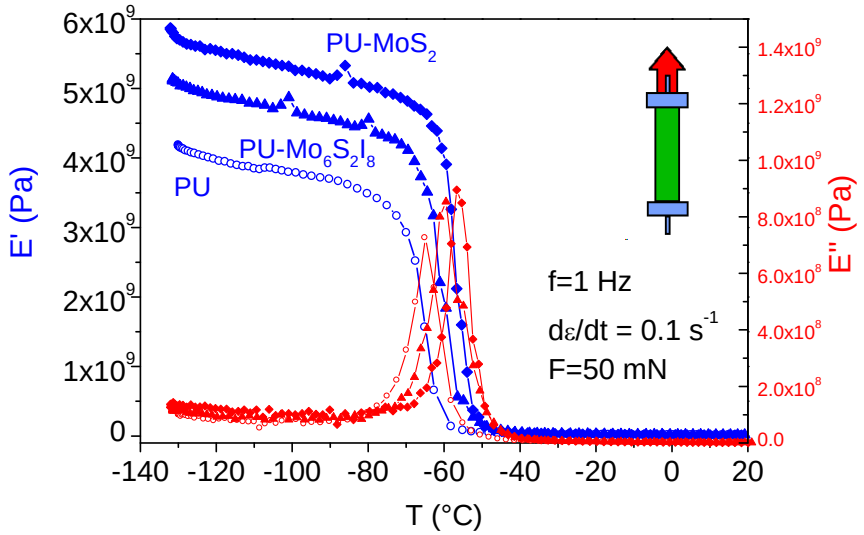

Fig. 4. Real (*E*') and imaginary (*E*") part of the complex Young's modulus for the pure polyurea elastomer (PU) and the two nanocomposites (PU-MoS_2 and PU-$Mo_6S_2I_8$).

Table 3. Glass transition temperature (T_g) and shift of the glass transition temperature (ΔT_g) for the polyurea elastomer (PU) and the two nanocomposites (PU-MoS_2 and PU-$Mo_6S_2I_8$).

	T_g (°C) (DMA)	ΔT_g (°C) (DMA)	T_g (°C) (TMA)	ΔT_g (°C) (TMA)
PU	-65		-68	
PU-$Mo_6S_2I_8$	-60	+5	-62	+6
PU-MoS_2	-56.5	+9	-60	+8

For the nanocomposite with nanotubes (PU-MoS_2), an increase in the Young's modulus up to 15 % was observed in the whole measured temperature range, while for the nanocomposite with nanowires (PU-$Mo_6S_2I_8$) was up to 12 %.

The reinforcement of a polymer nanocomposite crucially depends on the polymer-nanoparticle interfacial interaction, the modulus of the filler component, the shape of the filler as well as the relative orientation of the filler particles with respect to the applied stress [19].

Assuming a simple law of mixture we can estimate the Young´s modulus E_c of the composite as

$$E_c = E_p(1-\phi_f) + E_f\phi_f, \tag{3}$$

where E_p and E_f are the Young´s moduli of the polymer matrix and filler, respectively and ϕ_f is the volume fraction of the filler.

With $\phi_f \approx 0.01$, $E_p(-120°C) = 4$ GPa and $E_f(MoS_2) \approx 120$ GPa [20], we obtain $E_c \approx 1.3E_p$, thus a reinforcement of ≈ 30 % is obtained for the PU-MoS_2 nanocomposite. Using the more elaborated Halpin-Tsai model [21] and an aspect ratio (length/thickness) of the inorganic nanotubes or nanowires of ≈ 100, we obtain even better agreement with our data from Fig. 4: $E_c \approx 1.16E_p$.

However, similar as for the thermal expansion coefficient α, a more quantitative analysis of the reinforcement effect of PU-MoS_2 and PU-$Mo_6S_2I_8$ needs additional knowledge about the polymer-nanotube interaction and the value of the Young´s modulus of the PU-nanoparticle system.

Having a close look to the DMA experiments, a second relatively broad peak (T_{g2}) at slightly higher temperatures in the tanδ profile (or equivalently in the loss modulus, E") was found in addition to the T_{g1} (Fig. 5). The origin of this second peak or shoulder will be discussed in the next section. It seems that this broad peak is related only to the polyurea matrix, since it appears already in the reference system (PU).

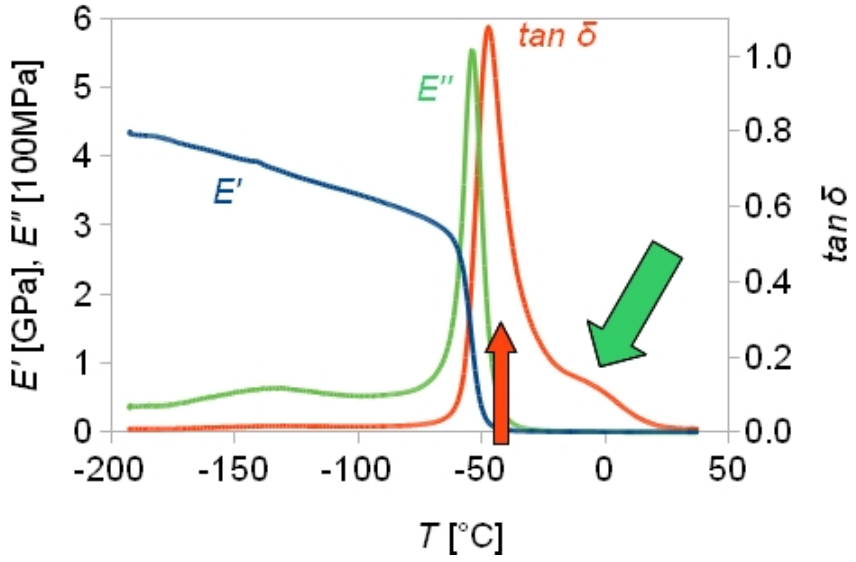

Fig. 5. Young's modulus E' (blue line), tanδ (red line) and E'' (green line) for the pure polyurea matrix (PU) measured in TS mode. The read and green arrows show the two glass transitions at T_{g1} and T_{g2}, respectively.

4. Discussion

The most significant findings of the present work on inorganic nanotubes-elastomer nanocomposites are the upshift of the glass transition temperature T_g with addition of nanoparticles, as well as the occurrence of a second peak or shoulder in tanδ and E" above the T_{g1} peak already observed in pure elastomeric matrix and both nanocomposites. Molecular dynamics simulations have shown [11] that the presence of nanoscale structures in the polymer network affects the glass transition temperature due to a change of the polymer dynamics. In the case of attractive interactions between the polymer and the nanoparticles, the chain relaxation time is increased and leads to a higher T_g relative to the pure system. For non-attractive interactions, a slight downshift in T_g is expected. Such influence of nanoparticles to polymer chain dynamics and glass transitions was indeed experimentally verified [12]. In our case, an attractive interaction between the polymer chains and the MoS_2 nanotubes and $Mo_6S_2I_8$ nanowires should then be proposed to explain the observed increase in T_g relative to the pure polyurea elastomer.

The second peak observed above T_{g1} in tanδ and in E" (Fig. 5) was also observed in the reference sample (PU). Therefore, it cannot be attributed to the presence of inorganic nanoparticles. However, as mentioned above even pure polyurea is a heterogeneous material consisting of hard nanodomains embedded in a soft matrix. It was shown [13] that such systems can exhibit *two glass transitions* at two different temperatures $T_{g1} < T_{g2}$. If the nanodomain-chain interactions are strong enough, the polymer chains near to a nanodomain exhibit reduced mobility compared to the regions far from the nanodomain. According to the so called EHM model [14], the second glass transition temperature at T_{g2} starts to be detectable when the regions of restricted mobility overlap, i.e. when the distance between nanodomains goes below the limit of about 5 to 10 nm. Then, the regions of reduced mobility

can undergo their own glass transition, since the value of 5 to 10 nm is approximately the size of dynamically correlated regions of glass forming polymers or liquids near T_g [15]. In previous works [2-4], the microphase separated domains were measured by means of SAXS, and the authors found distances of d =5.2nm. Thus, this second glass transition at T_{g2} might well be explained in terms of the nanoconfined hard domains in the polyurea elastomer.

The finding of a second peak in tanδ and E" is reminiscent of our recent results in a physically and chemically different but topologically similar system, i.e. the study of molecular liquids (salol, toluene, ortho-terphenyl, etc) confined in mesoporous Vycor and Gelsil with pore sizes between 2.5 nm and 10 nm [16, 17]. Here the restricted mobility of the molecules occurs due to an attractive interaction of the molecules near the pore walls, since the molecules form hydrogen bonds with the hydroxyl groups of the silica surface. Due to the dynamically decoupled motions of molecules far from the pore walls (faster motion → T_{g1}) and near the pore walls (slower motion → T_{g2}), two tanδ peaks could be clearly resolved for pore diameters bigger than 5 nm [16]. By silylating the surface of the pores, we could suppress the pore wall-molecule interaction and also the second glass transition temperature vanished [18].

5. Conclusions

We have presented thermomechanical and dynamic mechanical measurements on a polyurea elastomer and polyurea nanocomposites doped with inorganic nanotubes (MoS_2) and nanowires ($Mo_6S_2I_8$). The addition of nanoparticles causes a rather strong (up to 15 %) increase in the Young's modulus in the whole measured temperature range (from -130 °C to 20 °C), as well as an increase in the thermal expansion above the glass transition temperature T_g. The thermal expansion below T_g is unaffected by the presence of nanoparticles. The same behavior was also found in polyisoprene nanocomposites doped with carbon black (CB) and multiwall carbon nanotubes (MWCNT).

Adding inorganic nanoparticles to a polyurea matrix leads to an increase in the T_g, implying an attractive interaction between the nanoparticles and the polymer. An attractive interaction is also consistent with the observed remarkable reinforcement of PU-MoS_2 and PU-$Mo_6S_2I_8$.

A significant feature was the observation of a second broad peak in tanδ and E" above the glass transition temperature peak in pure and in doped samples. Since this second damping peak is also observed in pure polyurea, we argue that this second glass transition is occurring in regions near to the hard nanodomains. According to the arguments presented above, a separated second glass transition temperature can only be observed if the average distance between the hard nanodomains is not larger than 5 to 10 nm, as has been actually measured (d = 5.2 nm) for this system [2-4].

Although many interesting results have been found here for pure polyurea and polyurea/nanotube or polyurea/nanowire composites, clearly more measurements on well characterized samples with a larger range of doping concentrations are needed to reach final conclusions.

Acknowledgements

The present work was performed in the frame of the COST Action MP0902 (COINAPO – Composites of Inorganic Nanotubes and Polymers).

References

[1]. T. Hanemann and D. V. Szabó, Polymer-Nanoparticle Composites: From Synthesis to Modern Applications, *Materials*, Vol. 3, 2010, pp. 3468-3517.

[2]. A. Sánchez-Ferrer, R. Mezzenga, H. Dietsch, Orientational Behavior of Ellipsoidal Silica-Coated Hematite Nanoparticles Integrated within an Elastomeric Matrix and its Mechanical Reinforcement, *Macromol. Chem. Phys.,* Vol. 212, 2011, pp. 627-634.

[3]. A. Sánchez-Ferrer, M. Reufer, R. Mezzenga, P. Schurtenberger, H. Dietsch, Inorganic-Organic Elastomer Nanocomposites from Integrated Ellipsoidal Silica-Coated Hematite Nanoparticles as Crosslinking Agents, *Nanotechnology*, Vol. 21, 2010, pp. 185603/1-7.

[4]. A. Sánchez-Ferrer, D. Rogez and P. Martinoty, Synthesis and Characterization of New Polyurea Elastomers by Sol/Gel Chemistry, *Macromolecular Chemistry and Physics,* Vol. 211, 2010, pp. 1712-1721.

[5]. M. Remskar, A. Mrzel, Z. Skraba, A. Jesih, M. Ceh, J. Demsar, P. Stadelmann, F. Lévy and D. Mihailovic, Self-Assembly of Subnanometer-Diameter Single-Wall MoS_2 Nanotubes, *Science,* Vol. 292, 2001, pp. 479-481.

[6]. A. Kis, G. Csanyi, D. Vrbanic, A. Mrzel, D. Mihailovic, A. J. Kulik and L. Forró, Nanomechanical Investigation of $Mo_6S_{9-x}I_x$ Nanowire Bundles, *Small,* Vol. 3, No. 9, 2007, pp. 1544-1548.

[7]. M. Knite, V. Tupereina, A. Fuith, J. Zavickis and V. Teteris, Polyisoprene – multi-wall carbon nanotube composites for sensing strain. *Mat. Sci. Eng*., C, Vol. 27, 2007, pp. 1125-1128.

[8]. K. P. Menard, Dynamic Mechanical Analysis, *CRC Press, Taylor & Francis Group,* 2008.

[9]. E. K. H. Salje and W. Schranz, Low amplitude, low frequency elastic measurements using Dynamic Mechanical Analyzer (DMA) spectroscopy, *Z. Kristallographie*, Vol. 226, 2011, pp. 1-17.

[10].J. Yi, M. C. Boyce, G. F. Lee and E. Balizer, Large deformation rate-dependent stress-strain behavior of polyurea and polyurethanes, *Polymer*, Vol. 47, 2006. pp. 319-329.

[11].F. W. Starr, T. B. Schroder and S. C. Glotzer, Molecular Dynamics Simulation of a Polymer Melt with a Nanoscopic Particle, *Macromolecules*, Vol. 35, 2002, pp. 4481-4492.

[12].H. Oh and P. F. Green, Polymer chain dynamics and glass transition in athermal polymer/nanoparticle mixtures, *Nature Materials*, Vol. 8, 2008, pp. 139-143.

[13].G. Tsagaropoulos and A. Eisenberg, Dynamic Mechanical Study of the Factors Affecting the Two Glass Transition Behavior of Filled Polymers, Similarities and Differences with Random Ionomers. *Macromolecules*, Vol. 28, 1995, pp. 6067-6077.

[14].A. Eisenberg, B. Hird and R. B. Moore, A New Multiplet-Cluster Model for the Morphology of Random Ionomers, *Macromolecules*, Vol. 23, 1990, pp. 4098-4107.

[15].E. Hempel, G. Hempel, A. Hensel, C. Schick and E. Donth, Characteristic Length of Dynamic Glass Transition near *T*g for a Wide Assortment of Glass-Forming Substances, *J. Phys. Chem. B,* Vol. 104, 2000, pp. 2460-2466.

[16].J. Koppensteiner, W. Schranz and M. R. Puica, Confinement effects on glass forming liquids probed by dynamic mechanical analysis, *Phys. Rev. B*, Vol. 78, 2008, pp. 054203-1 – 054203-9.

[17].J. Koppensteiner and W. Schranz, Dynamic Mechanical Analysis of Confined Glass Forming Liquids, *Phase Transitions*, Vol. 83, 2010, pp. 744-757.

[18].J. Koppensteiner, W. Schranz and M. A. Carpenter, Revealing the pure confinement effect in glass-forming liquids by dynamic mechanical analysis, *Phys. Rev. B*, Vol. 81, 2010, pp. 024202-1 – 024202-8.

[19].G. D. Sims and W. R. Broughton, In: Polymer Matrix Composites, *Elsevier,* Oxford, 2001.

[20].A. Kis, D. Mihailovic, M. Remskar, A. Mrzel, A. Jesih, I. Piwonski, A. J. Kulik, W. Benoit and L. Forró, Shear and Young´s Moduli of MoS_2 Nanotube Ropes, *Adv. Mater.,* Vol. 15, 2003, pp. 733-736.

[21].J. C. Halpin and J. L. Kardos, The Halpin-Tsai Equations: A Review, *Polym. Eng. Sci*., Vol. 16, 1976, pp. 344-352.
